Title of Investigation: Preparing for DKIST - Science from NIR MCAO and Prominence AO in BBSO

PI: Philip Goode, BBSO/NJIT; **Co-PIs:** Thomas Rimmele, Dirk Schmidt, Vasyl Yurchyshyn and Wenda Cao
Collaborators: Thomas Berkefeld

A. Project Summary

Overview: Adaptive optics (AO) is the enabling technology for the 4 m aperture Daniel K. Inouye Solar Telescope (DKIST) with its AO corrected light to be fed to its sophisticated post-focus instrumentation. The 1.6 m Goode Solar Telescope (GST) in Big Bear is already equipped with state-of-the-art AO correcting light fed to its spectro-polarimeters. *The comparably designed GST is the ideal testbed for DKIST − both telescopes have an off-axis design with no obstructions in the optical path. The GST with its AO and its spectro-polarimeters make it a unique motivating pathfinder for early science goals utilizing the DKIST's instrumentation.* The AO part of the work proposed here builds on a nearly two decade long collaboration among Big Bear Solar Observatory (BBSO), the National Solar Observatory (NSO) and the Kiepenheuer Institut für Sonnenphysik (KIS) in Germany. Third generation visible light AO, multi-conjugate AO (MCAO), has enjoyed first successes in Big Bear in visible light utilizing three deformable mirrors (DMs) in which the corrected field was often trebled over that of a single DM (see *https://cuna.nso.edu/clear*) − wide-field correction is essential for DKIST. MCAO is vital for DKIST because the science is driven by the quest for the widest field, highest spatial and temporal resolution observations. Powerful, dynamic, magnetically driven events on the Sun can cover a $\sim 1'$ field of view (FOV) with seeming simultaneity, so measuring events requires temporal image stability over the FOV. Here we propose to expand upon the initial NIR MCAO developments, done on the GST, to further widen the corrected field (isoplanatic patch increases with wavelength) and collect/analyze/interpret the resulting scientific data collected with GST near infrared (NIR) instruments, which are forerunners of their DKIST counterparts (see *http://dkist.nso.edu/CSP*). Further, DKIST plans another, new kind of single DM AO − prominence AO, which has enjoyed initial success on the GST by correcting light just off the limb of the Sun, but much scientific probing remains to be done in these new territories for MCAO and AO leading into DKIST. We propose to sharpen the scientific motivations and AO iteratively for these early DKIST operations with preliminary, guiding research in BBSO using the GST as a stalking horse for DKIST. To aid the process, the data from all of the work we propose here will be immediately available to the community with special emphasis here for members of the DKIST Science Working Group (SWG). As well, a substantial portion of GST observing are open to the community, which may be of even greater interest and use in the DKIST era.

We propose three broad scientific tasks. Two utilize NIR-MCAO and the GST NIR-imaging-spectro-polarimeter (NIRIS) and the third utilizes our specialized single DM AO system for prominence AO. NIR-MCAO is designed to correct $70''$ and feed the $85''$ dual Fabry-Pérot NIRIS to produce high cadence imaging ($\sim$15 frames/s with 15 ms exposures) and vector magnetograms ($\sim$60 s cadence). The high cadence images will be used to track magnetic flux transport and diffusivity on small and large scales to probe the nature of of the local turbulent dynamo and global solar dynamo. The wide-field vector magnetograms from NIRIS will be used will be used to study photospheric and chromospheric waves and probe coronal heating. The single DM off-limb Hα AO will be used to study the elusive small-scale structure of solar prominences, as well as basic questions as to how plasma is supplied to prominences and how they evolve, and what is the nature of the Rayleigh-Taylor instability and does it play a role in supplying mass?

Our basic approach is to continuously improve both the NIR-MCAO and off-limb AO (both are new technologies) using, in part, the scientific data as feedback in an iterative fashion. In sum, we address two required criteria:
(1) Intellectual merit: It is critical to optimize the two new solar AO systems − NIR-MCAO and off-limb, prominence AO, both pathfinders for DKIST − and use their light feed for DKIST-like spectro-polarimeters to provide guidance for early DKIST science. After the DKIST is on-line, the GST will continue to be a critical telescope in making campaign-style observations.
(2) Broader Impact: NIR-MCAO and off-limb AO implementation and resulting science will provide useful data to the community, especially the DKIST Science Working Group for further and early elucidation of DKIST science opportunities. The resulting data from the upgraded GST will be used in many Ph.D. theses. Our data, and a substantial portion of GST observing will be open to the community. MCAO in the NIR is *terra incognita* in solar astronomy, but well-developed in the NIR Gemini South MCAO system (GeMS). Thus, the NIR MCAO observations proposed here are also relevant for nighttime telescopes.

B. Project Description

B.1 Broader Impacts

Adaptive optics (AO) is the enabling technology for the 4 m off-axis aperture Daniel K. Inouye Solar Telescope (DKIST) with its AO corrected light to be fed to its sophisticated post-focus instrumentation. With its three deformable mirror (DM) multi-conjugate AO (MCAO) operating in visible light on the 1.6 m offf-axis Goode Solar Telescope (GST) in Big Bear Solar Observatory (BBSO), the corrected field of view (FOV) was often trebled over that of a single DM (Schmidt et al., 2017) $--$ wide-field correction is essential for DKIST. Among DKIST AO light feed plans are MCAO in the near infrared (NIR) and prominence AO correcting Hα light just off the limb of the Sun, but *much scientific probing remains to be done in these new territories for MCAO and AO leading into DKIST*. The scientific motivations for these early DKIST operations will be sharpened from preliminary, guiding research in BBSO using the GST as a stalking horse for DKIST. To aid the process, the data from all of the scientific work we propose here will be immediately available to the community with special emphasis here for members of the DKIST Science Working Group (SWG). As well, a substantial portion of GST observing are open to the community, which may be of even greater interest and use in the DKIST era.

The GST was the first facility-class solar telescope built in the U.S. in a generation and has been in regular operation for a decade. The GST has single deformable mirror (DM) classic AO (CAO) and ground-layer AO (GLAO) in regular operation with three DM MCAO in a test phase in visible light. MCAO in the NIR is *terra incognita* in solar astronomy, but well-developed in the NIR Gemini South MCAO system (GeMS). Thus, the NIR MCAO observations proposed here are also relevant for nighttime telescopes. Further, we propose science utilizing single DM in a new way, off-limb AO to study prominence dynamics, and our work here will be a pathfinder for DKIST off-limb AO.

B.2 Overview of AO $--$ the Enabling Technology

The advent of Adaptive Optics (AO) has revolutionized solar astronomy by enabling diffraction limited observations of our nearest star. Until now, the stunning successes of solar AO have come from systems with a single DM, configured so that only the isoplanatic patch (typically $\lesssim 10''$ in visible light under good seeing conditions) can be corrected to the diffraction limit with decreasing correction as distance from the patch increases. It is important to bear in mind, as the designers of DKIST did, that magnetic field dynamics are the cause of the sun's powerful, explosive and non-local events, like flaring and coronal mass ejections (CMEs), which can cover upwards of $\sim 1'$ or more (see Fig. 1). Spectro-polarimetric measurements of magnetic fields require imaging that is temporally stable over the entire field-of-view (FOV). Furthermore, a single cell of supergranular convection, the convective flow pattern that reflects the organization of the magnetic network of the Sun, is $\sim 30''$ in diameter. Thus, to study dynamic, magnetic reconnection events in the network boundaries, it would be invaluable to have diffraction limited resolution over a FOV that covers two network cells in spatial extent. The vast majority of solar observing programs would benefit tremendously from diffraction limited resolution over an extended FOV. For instance, a typical sunspot might cover $\sim 1'$ or more, which is about half the size of DKIST's FOV and about two-thirds the size of the FOV of the GST in the NIR. If a small-scale flare were to occur somewhere in the FOV, it is not likely that the flare would occur within the isoplanatic patch. Typically, image reconstruction is used to correct the full field to the diffraction limit at the cost of temporal resolution being reduced by a factor of $\sim$100, which yields time steps of a few seconds, rather than a few tens of milliseconds (ms) because the information in a burst ($\sim$100) of images is combined into a single image, whereas the images input to reconstruction are regarded as having roughly the same time scale as the dynamical action, for a review see Nordlund et al. (2009). Furthermore, dynamical solar phenomena, like flares (see Fig. 1) and CMEs, as mentioned, are quite non-local, with nearly simultaneous, somehow interconnected manifestations of the dynamics often spread over the entire FOV. Such large-scale events are tied to the origins of what is broadly called "space-weather" (for details see *http://swpc.noaa.gov*), which can impact the

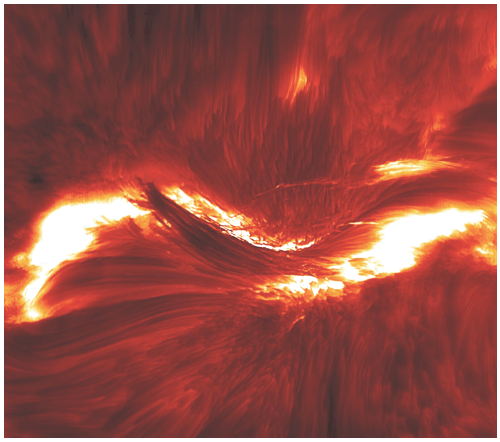

Figure 1: *Flare seen in chromosphere in Hα centerline. The GST image is for NOAA Active Region 11817 on 11 August 2013 and the FOV of $50'' \times 50''$ is spanned by the C2.1 flare's impulsive phase. Post-flare loops can be seen running right-left covering parts of the right-left flare emissions.*

terrestrial environment including satellites. *Since meaningful image reconstruction relies on an unchanging FOV during each burst, the reconstruction is problematic during the most scientifically significant moments of large dynamical events*. As well, MCAO image stability is essential for spectro-polarimetric inversions to obtain the large-scale evolving vector magnetic field. Thus, wide-field, diffraction-limited correction of MCAO is the holy grail for addressing the fundamental dynamics of our star with DKIST.

MCAO would provide the much needed real-time diffraction limited imaging over an extended FOV (Dicke, 1975; Beckers, 1988; Ellerbroek, 1994; Ragazzoni et al., 1999; Rigaut et al., 2000; Tokovinin et al., 2001). In the simplest view of MCAO, one has two, or more, deformable mirrors (DMs) to correct anisoplanatism with each DM being conjugated to a different layer of atmospheric turbulence. MCAO is a demonstrated technique for correcting atmospheric turbulence over a wide FOV for observations of the night sky (Marchetti et al., 2003; Rigaut et al., 2014; Neichel et al., 2014b), and the Gemini South MCAO system (GeMS) is routinely used for NIR astronomical observations (e. g. Neichel et al., 2014a). Wavefront sensing in nighttime MCAO is difficult because for general use, multiple laser guide stars (LGSs) are needed for tomographic wavefront reconstruction. Thus, to accurately reconstruct 3-D turbulence, generally a number of LGSs are needed. The Gemini South MCAO system (GeMS) uses five LGSs and three natural guide stars. This project was started in 1999, saw first light in 2011, and is now in regular operation. GeMS produces images close to the diffraction limit in the near infrared uniformly over a field of $2'$. Even though seeing tends to be better at night GeMs motivates NIR MCAO with DKIST so that scientists can hope to approach the full $2'$ FOV because terrestrial atmospheric turbulence is more benign in the NIR.

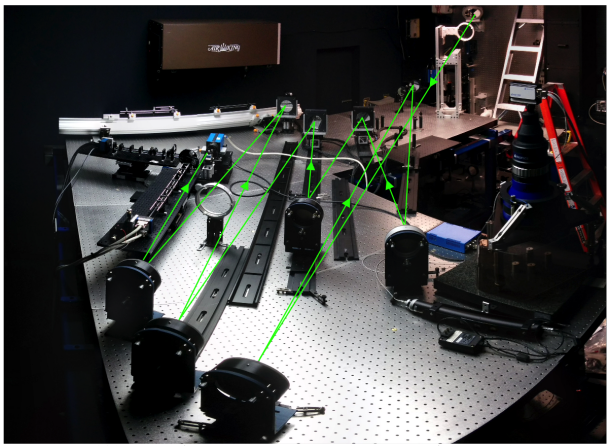

Figure 2: *The basic MCAO bench for Clear with the light path sketched in green (light enters from the upper right) and the 3 DMs side-by-side in the upper center of the figure. The black platforms on the left carry the multi-directional wavefront sensor (MD-WFS). Feed optics are not shown in this picture. The focal plane of the MCAO path is monitored with the large blue camera (PCO2000) next to the MD-WFS. The black dovetail rails allow for quick adjustments of the high-altitude DMs (see Fig. 3).*

The sun is a natural target for extended object wavefront sensing; any number of "guide stars" can be made from the 2-D structure of the Sun by using correlations from Shack-Hartmann wavefront sensing, which is the technique being used in our approach to solar AO. Implementing operational solar MCAO has been an essential, but challenging task that faces the GST, Gregor (the 1.5 m on-axis solar telescope built by our partners at KIS and deployed in Tenerife) and ultimately the DKIST.

The development of MCAO for existing solar telescopes and, in particular, for the next generation large aperture solar telescopes is stated as a top priority in the US adaptive optics roadmap (see http://aura-astronomy.org/nv/AO_Roadmap_2008 Final.pdf). The Sun is an ideal object for the development of MCAO since solar structures provides "multiple guide stars" with any desired configuration. *The roadmap further states that MCAO development must progress beyond these initial proof-of-concept experiments and should include laboratory experiments and on-sky demonstrations under controlled or well-characterized conditions, as well as quantitative performance analysis and comparison to model predictions. With our proposal, we respond fully to the US AO roadmap and propose to implement its goals for MCAO studies of the Sun in the NIR as applied to the GST and later to DKIST for science.*

Owing to its proximity, the Sun presents an extended FOV, and with its granular structure and various scales of magnetic features (in addition to MCAO correction of a granular field in TiO in Fig. 4, one can see G-band and active region MCAO corrected field in Schmidt et al. (2017) and more detail in *https://cuna.nso.edu/clear* HOW TO MAKE THIS CLICKABLE???), there are innumerable so-called "guide regions" (solar equivalent of guide stars, but guide regions are also extended objects, like granules, pores, etc.). Thus, the sun offers enough information to reconstruct the optical turbulence in earth's atmosphere even though it is a single star. The feasibility of solar MCAO was demonstrated in pioneering experiments (Berkefeld et al., 2010; Rimmele et al., 2010), which demonstrated that two DMs with up to four guide regions could reduce the residual image motion, and thus, in principal, effectively expand the corrected FOV.

Our MCAO system on the GST is called *Clear* and features an optical system with three DMs (see Fig. 2) and one or two wavefront sensors (WFSs). The peculiar looking optical design of *Clear* was made to allow maximum

flexibility in prompt individual adjustments in the conjugation altitude of each high-altitude DM due to our anticipation of evolving localized terrestrial atmospheric turbulence layers (see Fig. 3). The control system, KAOS Evo 2, for *Clear* was originally developed by Berkefeld and Schmidt for the Gregor telescope (Berkefeld et al., 2012). Here, we propose to use a more advanced version of that real-time control system, KAOS Evo 2, to continue the nearly twenty year long collaboration in AO among the BBSO of New Jersey Institute of Technology (NJIT), NSO, and KIS (hence KIS AO control system has the name KAOS) team, which has been supported by NSF. *Clear* includes MCAO, as well as two single DM systems, classical AO (CAO) and ground-layer GLAO (AO). For our purposes here *Clear*-NIR has been developed and lab-tested for exploration using MCAO in the NIR. Further, a new version of CAO has been developed and is being advanced for locking on prominences. Both systems will be used to lay groundwork for DKIST science with interactive, iterative improvement of the adaptive optics and scientific data.

B.3 Results from Most Recent and Closely Related Prior NSF Support

Initially we started our efforts in visible light with two separate wavefront sensor stages, namely an on-axis, high-order, narrow-field wavefront sensor (OA-WFS) and a low-order, wide field (or multi-directional) MD-WFS, which were built for a correctable FOV of 70″, following the MCAO approach at the German Vacuum Tower Telescope (VTT) and Gregor (Berkefeld et al., 2010) with the idea being to add high altitude corrections downstream in the optical train to those from a single pupil conjugated DM. In large measure, our on-sky experiments failed because we tried to correct too wide a field. Then, we halved the FOV from 70″ to 35″ in order to reduce the generalized fitting error by making each high altitude DM effective over a greater (deeper) range of altitudes. According to Rigaut et al. (2000), a DM with actuators spaced by $d_{\rm act}$ can cover a range in height of

$$\Delta h_{\rm max} = 1.75\, d_{\rm act}/\theta, \qquad (1)$$

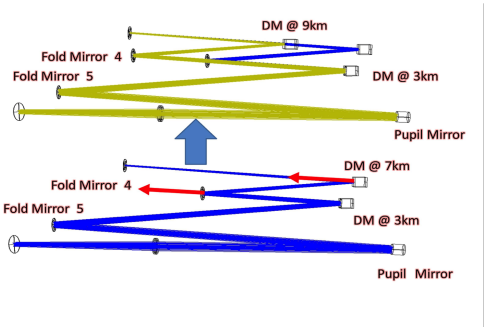

Figure 3: *Top: High-altitude DM is conjugated to 9 km. Below: that DM and its partner flat mirror are moved so the conjugation altitude is 7 km. No other optics need to be touched as long as the change is ±2 km.*

below and above the DM, with θ being the FOV to which the correction shall be applied. In our new case with about a 35″ FOV, this is approximately $1.75 \cdot 9$ cm$/30'' \approx 1$ km for the DM conjugate to the pupil, approximately 2 km for a DM when conjugate to 3 km, and about 3 km for a DM in 8 km. That is, with these specific conjugation altitudes of the three DMs, **we continuously cover the range from 0 to 11 km in visible light with the reduced wavefront sensing field of view**.

Narrowing the FOV in the visible, required implementing some new secondary optics. Concurrently, we had already planned to upgrade our low-order MD-WFS with a faster camera that would allow us to use more sub-apertures while preserving the FOV. With this camera, and the advised reduction of the FOV, we were able to design a medium to high-order MD-WFS that enabled us to eliminate the separate high-order narrow-field WFS that was required until then to appropriately cover the FOV. For the 2016 season, we implemented the new MD-WFS designs with 112 (11.8 cm) and 208 (8.8 cm) subapertures and a FOV of $35'' \times 35''$ that was divided among 7 or 9 guide regions, respectively. We ultimately used nine guide regions. Our new wavefront sensing scheme was very similar to the laser-guide-star scheme of the Gemini South MCAO System, which offers an equally high wavefront sampling for all 5 laser-guide-stars. The reconfigured MD-WFS also allowed us to operate the control loop in a medium- to high-order GLAO manner similar to that proposed by Rigaut (2002). The new wavefront sensor camera is able to read the 992×992 px needed for the 208 subaperture configuration at almost 1600 fps, however the real-time control computer that needs to process up to $208 \cdot 9 = 1872$ image correlations per loop cycle our control loop frequency was limited to about 1000 Hz, and thus also limited the control bandwidth for the 2016 observations, like those shown in Figs. 4 and 5. However, in Spring 2018 we replaced the control computer (under current ATI support) with one 50% faster and eliminated the control bandwidth concern. From the beginning, *Clear* was designed to have maximal opto-mechanical and real-time control system flexibilities to enable us to test various approaches that have been used, proposed, or could be adopted for solar MCAO, and to investigate the importance of the position of the pupil DM (e.g., before or after the high-altitude DMs, (Flicker, 2001)). For *Clear*, we use and advance the real-time control system KAOS Evo 2 to have maximal design flexibility for the iterative AO/science tasks proposed here.

Results from the **first ever clearly and easily visible successful solar MCAO imaging are shown in Fig. 4 (Schmidt et al., 2017)**. In this setup, the telescope light strikes the 8 km DM first, the 3 km DM second and pupil

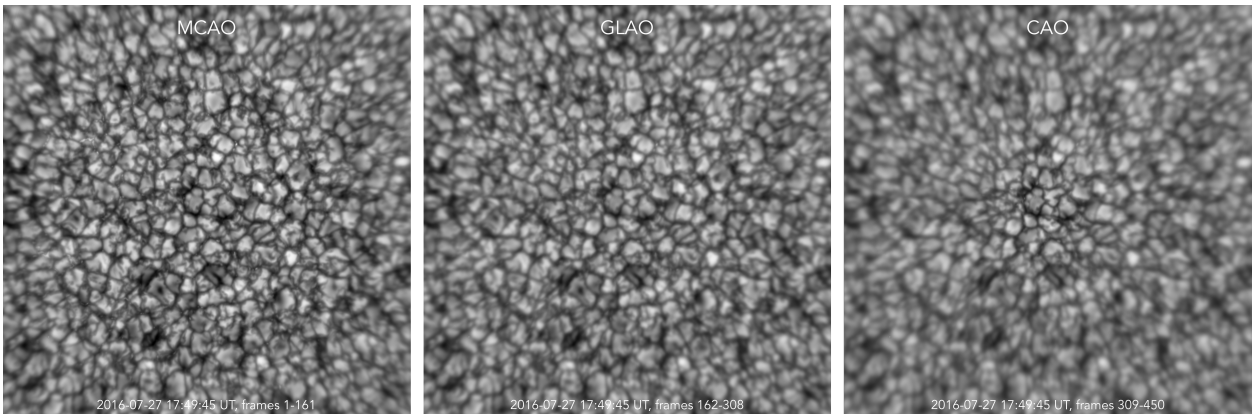

Figure 4: The Sun observed in a field of view of $53'' \times 53''$ with MCAO, GLAO, and CAO correction with *Clear* on the GST. The three images show a quiet region of the Sun between 10:49:45 and 10:50:16 PDT on July 27th, 2016 taken with a TiO filter (705.7 nm). Each image shows the sum of the raw, unprocessed frames within a block ($\sim$ 150 frames) with MCAO (left), GLAO (middle), and CAO (right) correction in a continuous burst of 450 frames recorded. Exposure time for was 1.6 ms for the granulation bursts and 11 ms for the sunspot. Real-time movies are available online at *https://cuna.nso.edu/clear* HOW TO MAKE THIS CLICKABLE???.

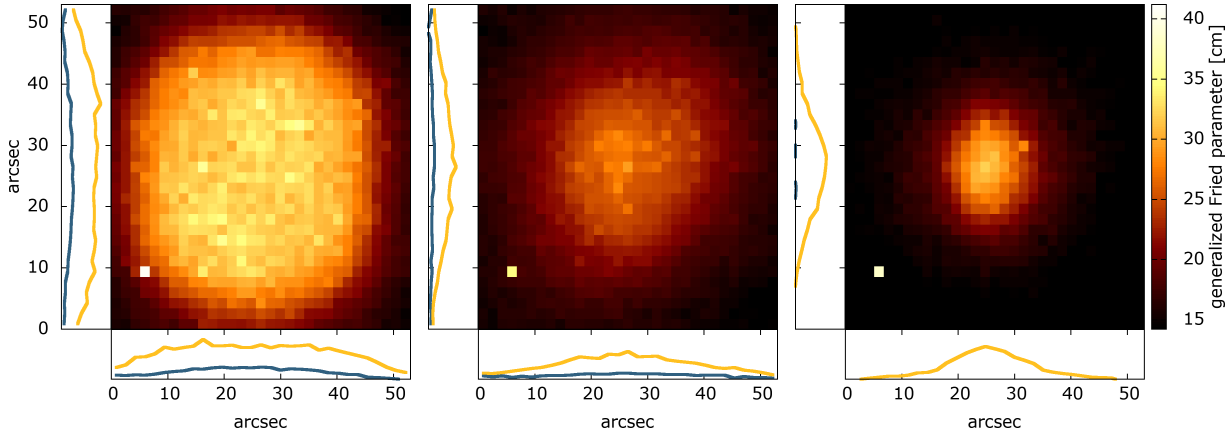

Figure 5: Generalized Fried parameter (Cagigal and Canales, 2000) across the field of view in the images shown in Fig. 4. The yellow lines along the ordinate and abscissa represent the relative intensities down and across the middle of the field, whereas the blue lines represent the corresponding relative intensities along the margins. For both rows, the full-width at half-maximum in the CAO yellow is $\sim 10''$, while that for the MCAO is $\sim 30''$.

DM last before the WFS. The results are from expired NSF-AST-ATI-1407597 support. These first step explorative, but impressive results were obtained on the GST with the a wavefront sensing FOV of $35''$ that utilizes a single multi-directional Shack-Hartmann wavefront sensor (MD-WFS), and nine guide regions over the FOV to be corrected on the Sun.

We chose to exploit the (Gemini South DM order) in our wavefront sensing scheme because the pupil DM would not be perturbed by the high-altitude mirrors. Further, it is easier to keep the alignment stable if the pupil DM (the one that sees the most turbulence) is near by the WFS. Last but not least, it's also the likely to be the easiest setup with which to integrate MCAO into DKIST. At any rate, these were the first on-sky MCAO solar images that show a clearly and visibly widened corrected field of view compared with quasi-simultaneous observations with single DM classical adaptive optics (CAO) correction. We have since made repeated observations and achieved comparable results with this optical setup.

With a total of 1071 actuators in the DMs of which 555 are effectively used at this time, *Clear* offers the most degrees of freedom for image correction of any solar telescope today (UPDATE PARAGRAPH FOR NIR SOMEWHERE LATER???). Each of the DMs, which were manufactured by Northrup-Grumman AOA Xinetics, has 357

actuators and shows a best flat figure error of about 4 nm rms. In order to identify the poorly reconstructed wavefront modes on the DMs, we used a simple analysis of the system's condition number. Depending on signal to noise conditions, we used typically about 150 Karhunen-Loeve modes on the pupil DM, and up to 90 and 50 modes on the DMs at 3 and 8 km, respectively, with the MD-WFS configuration having 208 subapertures and 9 guide-regions.

For some details, during our first very successful experiments that took place in July 2016, we monitored the focal plane with a CCD camera through an interference filter for the titanium oxide line (705.7 ± 5 nm). We took numerous bursts of 450 frames with short exposures operating at 14.7 frames per second, i. e. a total time span of approximately 31 seconds. Each burst typically contains about 150 frames (10 sec) with continuous MCAO, GLAO and CAO correction. (The KAOS Evo 2 control software enables us to switch the mode of AO correction instantaneously without losing lock.) These bursts are short enough to be interpreted as *quasi-simultaneous* observations with CAO, GLAO, and MCAO correction. In order to rule out that the perceived effects are due to unnoticeable seeing changes that happen to occur co-incidentally when we switched the mode of correction, we recorded numerous such bursts. In the CAO mode of correction, we used the pupil DM and the central guide-region only, the other DMs were at rest and off-axis guide-regions were ignored. In GLAO mode, we allowed all guide-regions to equally control the pupil DM, while the higher DMs were still at rest. From simultaneously recorded control loop telemetry data, we can identify the frames in each burst that were corrected in MCAO, GLAO, or CAO manner, respectively. The three images in Fig. 4 contain a total of the 450 frame bursts, recorded in July 2016, and divided into three comparably sized blocks of MCAO, GLAO, and CAO correction, where each image shows the superposed frames of each block.

In left panel of Fig. 4, the great improvement is obvious with $< 0''.2$ intergranular lane bright points (Goode et al., 2010) being easily apparent even at the edge of the $\sim 35''$ diameter corrected FOV $-$ the setup aimed for a $35''$ corrected FOV and achieved it. In these observations, as mentioned, nine guide regions were used. Results like those in Fig. 4 were seen many times in the ten day observing run near the end of July 2016 and in multiple runs during the Spring, Summer and Fall of 2017. Another way to understand Fig. 4 is to examine the generalized Fried parameter (Cagigal and Canales, 2000), which measures the increased generalized Fried parameter across the field due to the AO correction (see Fig. 5). We computed the generalized Fried using the KISIP image reconstruction software (Wöger et al., 2008). *It is noteworthy that the FOV in Fig. 4 is a granular field, which makes the results even more impressive because relatively low-contrast granulation is harder to lock-on than the rather high-contrast magnetic features like pores.* The rightmost panel of Fig. 4 shows superposed images gained with CAO correction. The relatively small isoplanatic patches are apparent near the center of the FOV of each. Inspection of Figs. 4 and 5 shows the improvement of MCAO, as well as the differences between between ground-layer and classical correction. One can see advantages for both CAO and GLAO depending on the requirements of the observations with CAO providing better image detail in a small FOV, while ground-layer correction resulted in a lower but more homogeneous image detail over the field compared to classical correction. During our experiments, however, we found that the effect of our GLAO mode of operation was not consistent from observation to observation. We anticipate a role for variable turbulence distribution to explain this. Overall, it is apparent that MCAO is a great improvement over CAO and GLAO. We note that we were able to operate the MCAO control loop stably whether the pupil DM was placed before or after the high-altitude DMs.

Among our previously NSF supported AO projects, the single DM system, AO-308, was supported by NSF-AST-ATI-0905279. AO-308 was the second generation AO system in BBSO. The DM has 357 actuators and 20 subaperatures across a diameter of the primary mirror implying 8 cm subapertures, which was sufficient for AO-308 observations to correct the bluest of visible light under good seeing. For DKIST the comparable DM has 1550 actuators! The AO-308 system was based on digital signal processors rather than PCs, as in *Clear*, for the wavefront sensing and DM actuator control. We found that KAOS on CAO functioned better than AO-308. AO-308 was used during ordinary observations and operated from a vertical bench, while the KAOS-based *Clear* system is a self-contained experimental system on a separate, horizontal optical bench. During regular observations in 2016 and 2017, a single DM is used and was devoted to AO-308, but during our work on *Clear* all three DMs are devoted *Clear*. The fact that experiments with AO-308 using the BBSO system and CAO using KAOS gave similar results was comforting and demonstrated the power of PCs in AO. In Spring 2018, we replaced AO-308 on the vertical bench by CAO, so that for the 2018 Summer observing season we had CAO and GLAO on the vertical bench feeding the spectro-polarimeters. Another motivation for the upgrade was that, the AO-308 WFS camera is several years old and was replaced as part of this upgrade to CAO on the vertical bench, as well the WFS camera used in *Clear* is cheaper and, with its greater well-depth, performs somewhat better than the AO-308 WFS camera.

The first generation AO system on the GST featured 97 actuators with 76 subapertures (10 along a diameter) with 16 cm subapertures along a diameter. This system could only correct light in the near-IR on the GST, but was sufficient for the old 0.5 m solar telescope in BBSO, which was retired a decade ago. This early AO work was supported by NSF-MRI-AST-0079482 nearly twenty years ago and led to first generation AO systems in Big Bear and on the Dunn

Solar Telescope (DST) of the National Solar Observatory (NSO). All three generations involved close collaboration between BBSO, NSO and KIS with Goode (BBSO) and Rimmele(NSO) being the only principals common to all AO and MCAO grants mentioned in this section.

The first MCAO setup in BBSO was built under NSF-MRI-0959187 support. The MCAO pathfinder *Clear* on the GST was built to address a multiplicity of design options with maximal flexibility because there are many outstanding issues in maturing the MCAO technology for solar observations. To our knowledge, *Clear* is not only today's most powerful solar MCAO system, but also currently the only MCAO system installed on a telescope and ready to look at the Sun, and certainly the only one to enjoy such a resounding success. The basic system features three deformable mirrors, each having 357 actuators and, as discussed, utilizing 9 guide regions and one wide-field WFS, although other options are readily possible (such as up to 19 guide regions with our control system). CAN SHORTEN THIS PARAGRAPH???

Our active MCAO grant is NSF-AST-1710809, which was submitted as an ATI proposal. The tasks proposed here are completely distinct from the technology tasks funded over a year ago in the two year grant NSF-AST-1710809, where the four technology tasks are: a) Develop a profilometer for DKIST and BBSO to determine the real-time atmospheric turbulence profile; b) Solve image distortion problem in reference image updating for *Clear*, *Clear* has held lock for extended periods (>1 hr) even with this problem; c) Use 4th DM to be loaned Northrup-Grumman to determine optimal order of MCAO 3 DMs in *Clear*; d) Implement a faster real-time control computer to get an improved treatment of fast turbulence. This last task has been successfully performed already, as mentioned above. Of course, there could be ancillary benefits for the work proposed here from these four tasks (like the implementation of task d)), but none of the work proposed herein depends on any of the four tasks, a) - d). Further, none of the four tasks in NSF-AST-1710809 draws any obvious benefits from the work proposed here.

C. Proposed Work

In preparation for the work proposed here, and in addition to all other GST AO work plans, we have implemented and tested engineering versions of MCAO in the near infrared (NIR) and prominence AO correcting light just off the limb of the Sun. Light from both these AO systems will be fed to GST focal plane instrumentation opening new scientific opportunities. Here we propose to perform these pathfinding explorations in which the AO-corrected light is fed to BBSO spectro-polarimeters that are forerunners to their counterparts on DKIST. In the NIR, where atmospheric turbulence is more benign, we have doubled the FOV to be corrected by MCAO to $70''$ to feeding light to the BBSO NIR spectro-polarimeter (NIRIS). In the NIR, for instance, we can lay the groundwork for the next generation of scientific exploration of the deepest part of the photosphere (near 1.6 μ) in which lines like one near 1.56 μ, with a Landé g-factor equal to 3, and the chromosphere elucidating 1083.0 nm light. With these, we can perform unparalleled studies of wide FOV solar dynamics. Second, we propose to utilize another new type of solar AO on the GST correcting just off the edge of the Sun on prominences. This is unexplored territory in which a single DM AO is locked on the Hα light from limb prominences. AO locking on prominence light is an appealing gateway to significantly improved probing of the Sun off-limb. However, this requires a different approach to AO. With a single DM locking on disk features, one uses broad-band light (525$\pm$12 nm), however a prominence would be about two orders of magnitude dimmer, and hence invisible/lost in broad band. Thus, off-limb, prominence AO forces one to a narrow-band (656.3$\pm$0.1 nm) design around the bright Hα light, but even then this is a photon-starved problem. In partial compensation, the prominence AO WFS has a FOV of about $25'' \times 25''$ (compared to about $10'' \times 10''$ for CAO) and prominence AO, or *Clear*-Prom, uses somewhat longer exposure times. Taylor et al. (2015) were the first to build a prototype of such a system. They used a narrow-band Hα prefilter that took all the prominence light feeding a Shack-Hartmann WFS with fewer subapertures than they would have used on-disk. Their work was performed on the Dunn Solar Telescope (DST). On the GST, we have already implemented a successful engineering grade version of their system that takes less than half of the Hα light under mediocre seeing conditions (see **C.3**). In Big Bear, we propose to feed the AO corrected light to FISS and VIS to measure different aspects of prominence dynamics by simultaneously measuring photospheric and chromospheric effects with our fast imaging solar spectrograph (FISS) and measure magnetic field dynamics with our visible light spectro-polarimeter (VIS). FISS can measure dynamics using Hα and CaII (854.2 nm) to simultaneously measure the photosphere and chromosphere. FISS and VIS detect phenomena that VBI, ViSP and VTF will probe on DKIST (see *http://dkist.nso.edu/CSP* for details of DKIST instrumentation and science goals).

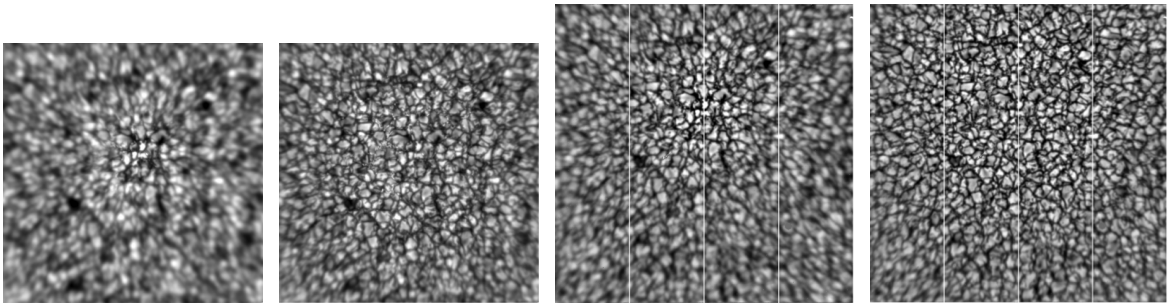

Figure 6: The two left panels are TiO (0.705 μ) and this spectral line intensifies bright points. TiO observations shown here have a FOV $\sim 50'' \times 50''$. The two right panels show simultaneous NIR observations at 1.56 μ. The first and third panels were obtained using CAO, while the second and fourth panels come from the same MCAO setup that led to Fig. 4 (correcting a 35″ FOV). A beamsplitter was used for CAO simultaneously with TiO and 1.56 μ and then switching to MCAO TiO and 1.56 μ, etc. 1.56 μ observations are of special interest because of the presence of the local g=3 line and the deepest photosphere is revealed in this wavelength regime. The NIR observations have a FOV $\sim 60'' \times 60''$. Each of the four panels is the uncorrected sum of $\sim$150 observations from October 27, 2017 on a day of mediocre seeing. All four panels have the center of the isoplanatic patch offset upwards to better show the roll-off in correction with distance from the patch. The vertical lines in the NIR observations are an artifact of read-out in BBSO's old 1k$\times$1k NIR camera that we used here for ease of operation.

C.1 Facilities: Current GST Instrumentation

As of this writing there are two AO systems on the GST. *Clear* resides on the horizontal bench and includes CAO, GLAO and MCAO. These three sub-systems are not yet connected to the GST instrumentation suite. The second system that was implemented Spring 2018 includes the thoroughly tested CAO and GLAO being placed on the vertical bench (replacing AO-308) feeding the current focal plane instrumentation. The GST optical systems and instrumentations (Goode et al., 2010; Cao et al., 2010; Goode et al., 2012) offer a significant improvement in ground-based, high angular resolution and polarimetric capabilities and were built with support from NSF. The GST post-focus instrumentation (see *http://www.bbso.njit.edu* for details) that we propose to use are:

Near InfraRed Imaging Spectro-polarimeter (NIRIS, Cao et al., 2011) is a dual Fabry-Pérot etalon system allowing us to fine tune to any wavelength between 1.0 and 1.7 μm. NIRIS's FPI etalons provide a large, 85″, FOV and high throughput resulting in a faster scan cadence of 1 sec for spectroscopic and 10 sec for full Stokes polarimetric measurements. The dual-beam optical design images two simultaneous polarization states onto a 2024x2048 HgCdTe closed-cycle He cooled IR array. The primary lines of interests for NIRIS are the Fe I 15650Å doublet, which is the most Zeeman sensitive probe of the magnetic field ($g = 3$) in the deepest photosphere and the He I 10830Å multiplet that is the best currently available for diagnostics of upper chromospheric magnetic fields. Here MCAO fed NIRIS will help to provide motivating results for DL-NIRSP on DKIST.

Visible Image Spectrometer (VIS) initially utilized an FPI etalon with a bandpass of 0.1Å with the possibility to shift the bandpass by 2Å around the Hα line center. The pixel scale is set to 0″.027 and the FOV is 69″ by 58″. A full line scan with a 0.2Å step (11 positions) can be performed with cadence of about 2 s between the positions. Images at one arbitrary position can be taken with a much higher cadence. VIS is currently being upgraded to a dual FPI, like NIRIS, to cover from 550 nm to 860 nm. The upgraded VIS should be online before the start of the work proposed herein.

Fast Imaging Solar Spectrograph (FISS Chae et al., 2013) is a field-scanning slit spectrograph with high spectral resolution (1.4×10^5) and scanning speed (10 s) able to sufficiently cover a FOV of $40'' \times 60''$. Two different major spectral lines such as Hα, Ca II H and K, and Ca II 854.2 nm can be recorded simultaneously using two CCD cameras, which allows one to distinguish between the thermal component and the non-thermal turbulence, so that a precise determination of temperature is possible. FISS was built for GST by our Korean colleagues. VIS and FISS will be used in prominence studies.

C.2 *Clear*-NIR with a Wide FOV

The corrected FOV with *Clear* is 35″, which is considerably smaller than the FOV of BBSO's NIR spectro-polarimeter, NIRIS (85″ diameter). The FOV for *Clear* in visible light was narrowed to 35″ so that the depth of field of the three combined DMs was sufficient to cover all altitudes from the ground to 11 km above the ground, which seemed to be

required for full, wide-field correction. For the NIR ($\sim$1.0-1.6 μ), our wide-field setup covers a FOV 70″, under the logical assumption that the seeing is Kolmogorov (turbulence decreases with wavelength as $\lambda^{\frac{6}{5}}$) so a larger actuator spacing can be used (see Eqn. (1)), yielding the same depth of field coverage with twice the FOV, which opens many scientific opportunities in the NIR, and comes close to filling the 85″ FOV of NIRIS.

As a first step to motivate NIR MCAO testing, we made proof-of-concept observations on October 27, 2017, under mediocre seeing, in which we used the 35″ *Clear* setup for which we fed the MCAO corrected light to a beam splitter that in turn simultaneously fed light to two different cameras sensitive to 0.705 μ and 1.56 μ (see Fig. 6), respectively. The isoplanatic patch of the images shown in Fig. 6 are off-center (offset toward the top of each image) to better illustrate the roll-off in correction away from the center of the patch. (Aside: the Rockwell camera has a smaller FOV than NIRIS - the Rockwell camera was used because it was easier to handle, so as to avoid separating the more modern NIRIS camera from NIRIS.) For single DM CAO, the much larger isoplanatic patch is apparent for the NIR. For MCAO, the wider correction and more gradual roll-off for the NIR is apparent, but the optics are for a 35″ corrected field. Nonetheless, the MCAO results serve to strongly motivate replacing the MCAO optics for visible light with ones appropriate for the larger field in the NIR. We have implemented the requisite optics in our setup on the horizontal bench, but to the eye the setup looks indistinguishable from Fig. 2. We tested this 70″ NIR MCAO setup on 2 October 2018 in several laboratory tests with an artificial target and turbulence generated by cooktops placed in front of each of the three DMs, the effectiveness of the wide-field correction can be seen in Fig. 7. And we will try this setup on-sky at our earliest opportunity. We gain further confidence by noting that this larger field would be more like (1′-2′) that used by GeMs in the NIR in which the field is corrected with two DMs on Gemini South. The design for connecting *Clear*-NIR to NIRIS is straightforward, simple and complete. Neither system will be moved, but rather the two are connected by three mirrors and two lenses (for design details see Appendix???).

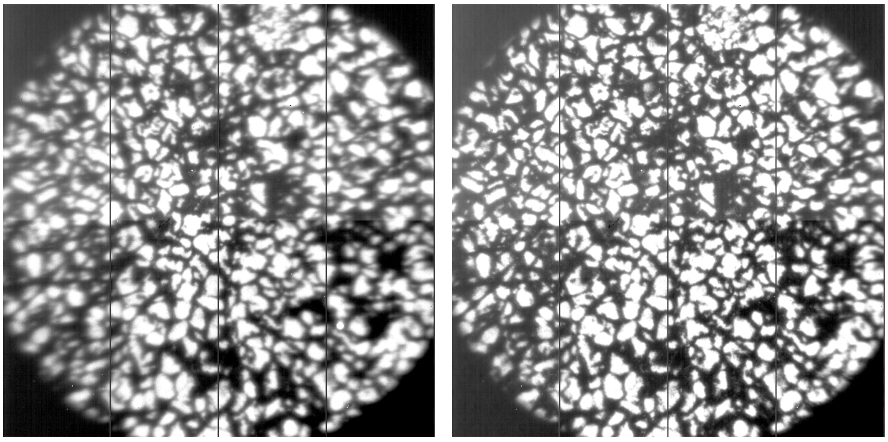

Figure 7: Superposition of $\sim$150 frames in 1.56 μm light from a lab target of granulation with a cooktop in front of each DM. CAO is on the left and MCAO is on the right. The optics is for a 70″ FOV but the camera has a 60″, hence the clipping. Nonetheless, lab test are encouraging. We used 55 KL modes on-axis and an additional 22 modes for wide field (OK????), but this was just a quick (and successful) test of our NIR MCAO optical setup.

C.3 Prominence AO (*Clear*-Prom) FIRST REFERENCE???

For *Clear*-Prom, initial testing of the hardware was done in the Spring of 2018 and repeatable results (Schmidt et al., 2018a,b) are shown in Fig. 8. In this engineering setup nearly 40% of the light went to the *Clear*-Prom WFS, while about 30% went to the VIS instrument and the remainder to the TiO camera. With this setup we were able to close the loop and hold lock to improve off-limb image quality under mediocre seeing conditions for a weak prominence on May 13, 2018. In Fig. 8, we show an average of about 100 on-band Hα images using VIS tuned to a narrow, line-center bandpass so that only a small part of the Hα light incident on VIS is used. Tip/tilt improved image quality and AO further significantly improved it near the center of the FOV, see Fig. 8 for a comparison of WFS errors, and, as usual for AO, wider-field correction is expected under better seeing. Thus, we are encouraged by results like those illustrated in Fig. 8. Many options are now open to us using *Clear*-Prom, for instance, we could replace VIS with FISS for ease of Hα/Ca II studies of prominence dynamics with a brand-new generation of resolution. Further, we will improve the

engineering setup before the proposed work begins, and iterative improvements will continue in conjunction with the proposed science.(WITH 12 SUB APERTURES CAN ONLY REACH NEAR THE DIFFRACTION LIMIT???)

Both MCAO in the NIR and prominence AO will provide corrected light enabling us to probe problems that have been beyond our grasp and the results will provide scientific guidance and motivation for DKIST, and the data will be used to cross-check the AO.

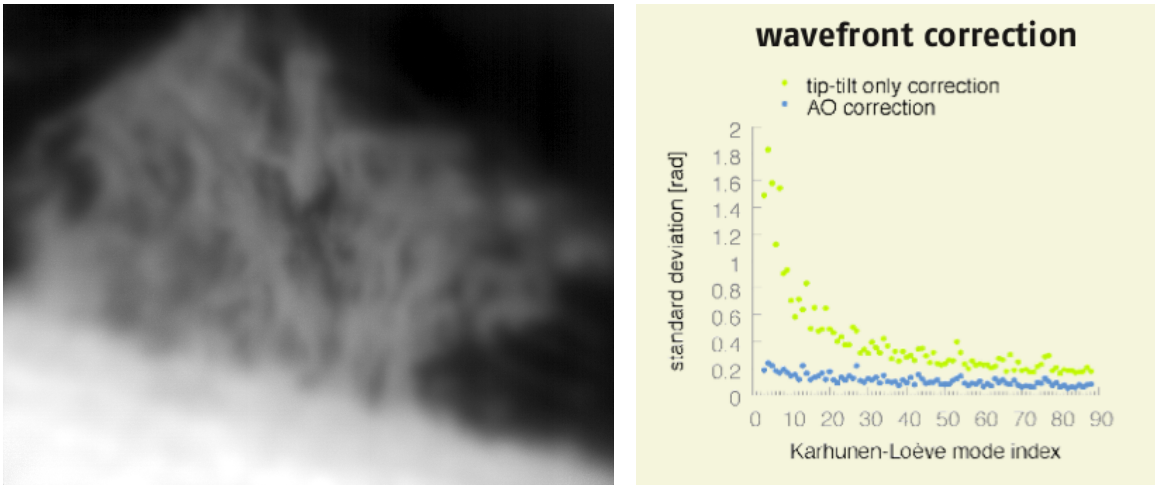

Figure 8: Superposition of ∼100 frames of Hα images corrected by (88 KL modes) *Clear*-Prom from Schmidt et al. (2018b). Left: Each exposure was 2 ms in duration in the ∼15 frames/s burst. The data were dark and flat field calibrated. The were taken on May 13, 2018 on a day of mediocre to poor seeing using VIS with a $50'' \times 50''$ FOV. Right: Beyond tip-tilt, the apparent AO correction was confined to near the center of the FOV, as one might expect under the seeing conditions in effect that day with central region having a significantly improved wavefront correction.

C.4 Magnetic flux transport and diffusivity

Introduction. The global solar dynamo and the local near-surface turbulent dynamo both manifest themselves via emergence and subsequent dispersal of new magnetic flux on the solar surface. To understand the dynamo process, one has to understand the dispersal of the magnetic flux, which is usually described in terms of magnetic diffusivity. The corresponding diffusion coefficient is usually considered to be a free parameter in the various models of solar dynamo and magnetic flux transport.

Our team proposes to explore the diffusivity process that occurs over a wide range of spatial and temporal scales by utilizing MCAO corrected GST magnetic field measurements in the NIR utilizing NIRIS − *Clear*-NIR. This research is motivated by our earlier discovery of a super-diffusivity regime in the quiet-sun photosphere on small spatial ($\leq$500 km) and short temporal (10 – 600 s) scales. Combining HMI and GST/TiO data, Abramenko (2017) found that the diffusion regime changes on temporal scales of 5-15 min and spatial scales of 0.30-2.0 Mm. *Is the super-diffusivity regime replaced by normal and/or sub-diffusion as the scale approaches the super-granular scale?* The problem is this range is not well-covered either by the current GST data (spatial scales too large) or HMI (time steps too low). Our goal is to extend the spectrum toward the upper end of both scales as far as possible (60-80 Mm) incorporating long time series of GST *Clear*-NIR wide-field, corrected magnetic field measurements. These will allow for accurate tracking of magnetic field elements on those key spatial scales.

More specifically, the task of this goal is to study diffusivity on various scales ranging from smallest ($<$1 Mm, $<$10 sec) and super-granular ($\approx$ 30 Mm) scales using *Clear*-NIR wide-field corrected data that would include a super-granular boundary. Note, that CAO can produce diffraction limited data only over a limited FOV of order of $20''$ in the NIR, which is much smaller than required.

Method. In general, the data required to estimate magnetic diffusivity are trajectories of some sort of tracers in a turbulent flow. In our case, the tracers will be either photospheric bright points (BPs) observed in broad band filter images (small spatial and temporal scales) or magnetic flux concentrations (larger, super-granular scales) seen in

photospheric magnetograms. Typical examples of BP trajectories as derived from GST data are shown in Figure 9. The position of a tracer along its trajectory can be measured at several discrete moments. Then spatial displacements of an individual tracer as a function of time can be calculated. Next, an average (over all tracers) displacement for each time interval is calculated to produce the average squared displacements ("drift" displacement spectrum) because it is obtained from a drift of single tracers.

Both advection and turbulent diffusion contribute into this drift spectrum. There are ways to significantly reduce the influence of advection and estimate the turbulent diffusivity utilizing a pair separation technique (Monin and Yaglom, 1975; Lesieur, 1990). Here, the displacements are computed as distances between two tracers at consecutive moments. Since large-scale advection is expected to affect both tracers equally, it is thus eliminated. This will allow us to estimate the interplay between advection and turbulent diffusion on various temporal and spatial scales.

On small scales we will track photospheric BPs, which are thought to be footpoints of magnetic flux tubes (e.g., Muller et al., 2000; Berger and Title, 2001; Ishikawa et al., 2007). Therefore, studying BPs make it possible for us to measure the dynamics of the photospheric magnetic flux tubes (e.g., Berger et al., 1998b,a; Cadavid et al., 1999; Lawrence et al., 2001; Utz et al., 2009). Only a fraction of magnetic elements (about 20%, de Wijn et al., 2008) are thought to be associated with BPs, therefore they allow us to study only a subset of the entire magnetic flux tube population.

BPs are automatically detected in all images and then tracked from one image to the next. Here we used the detection and tracking code previously described in Abramenko et al. (2010). Our method uses the same approach as that of Berger et al. (1998b,a), in which they selected BPs by applying thresholding and masking. When two elements merged, the tracking of the smaller one was terminated. We estimated the residual image jittering in the data set and found that it is very small and stable over the data set with an r.m.s. of 0.1 pixel (2.7 km) and a maximum value of 0.26 pixel. We therefore adopt the r.m.s. value of 2.7 km as a typical error of calculations of the BP position. More details on our tracking code can be found in Abramenko et al. (2010, 2011).

Tracking on supergranular scales will be done using the same numerical tool, however the object of tracking will be different. We will track absolute values of the line-of-sight magnetic flux densities. Applying a threshold of 30 G to HMI data, Abramenko (2017) detected 17312 flux concentrations and tracked only those that lived at least 3 timesteps or longer. We would like to emphasize that the above techniques were developed, tested and used by our groups in the past (Abramenko et al., 2010). Our main task here will be to collect a high quality data set and run the tracking routines to collect the data. This is the most challenging task. The tracking routine has been developed and tested and used, but we anticipate that we will need to fine tune it to the new data set that NIRIS will provide. After the tracking is finished, the generation of the displacement and separation spectra as well as estimates of magnetic diffusivity (see below) are straightforward and not time consuming.

The power index, γ, of a displacement spectrum allow us to derive dependence of the diffusion coefficient, K, on the spatial and temporal scales Monin and Yaglom (1975); Lesieur (1990). Our earlier works showed that the displacement spectra, obtained from GST/TiO quiet Sun data and from 3D MHD simulations exhibit well-pronounced power laws. We further concluded that the diffusion coefficient varies in direct proportion to the spatial and time scales (Abramenko et al., 2010).

We will expand the spectra toward i) small temporal scales by lowering time cadence of GST/TiO data and ii) larger spatial scales by expanding the analyzed area. Both requirements can be satisfied by using GST/NIRIS magnetic field measurements made with the aid of *Clear*-NIR that will allow us to expand the corrected FOV and lower the integration time.

C.5 Waves in the Chromosphere

Introduction. Alfven waves have long been proposed as a candidate mechanism to transport magneto-convective energy from the convection zone into the solar atmosphere where they can heat, through dissipation of their non-thermal energy, plasma to coronal temperatures (e.g., Belcher and Olbert, 1975; Axford et al., 1999). During the past few years, a variety of observations of Alfvenic waves in the chromosphere (e.g., De Pontieu et al., 2007; Okamoto et al., 2007), corona (Tomczyk et al., 2007; McIntosh et al., 2011) and even the photosphere (Fujimura and Tsuneta, 2009) have caused a resurgence of interest in these waves and their role in powering the solar atmosphere.

Most of the current observations of Alfven waves in the solar atmosphere are based on limb observations of spicules, plumes or other coronal features. As a result, it has been challenging to determine how and where these waves are generated. It remains unclear whether shuffling of strong magnetic field concentrations in the photosphere (e.g., Cranmer and van Ballegooijen, 2005), reconnection, or mode coupling (e.g., Newington and Cally, 2011) are the dominant source for these waves. The key to determining their formation mechanism is to observe them on the disk at

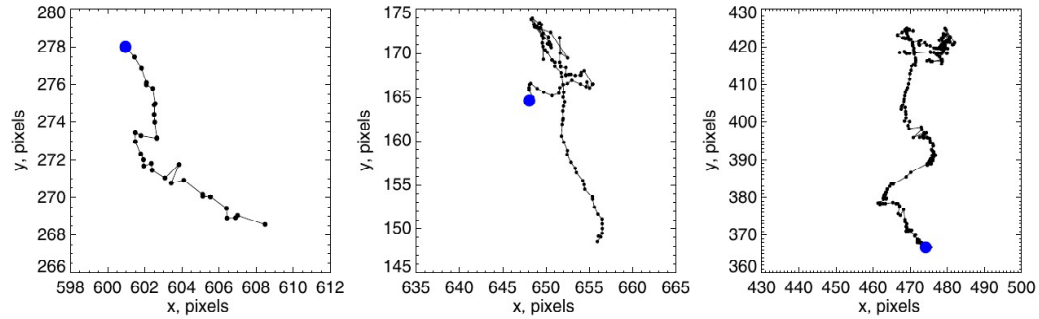

Figure 9: Typical trajectories of BPs.The time intervals between adjacent measurements (circles) is 10 seconds. Blue circles mark the start point of the trajectory.

their source, i.e., in the chromosphere.

Measurements of BBSO's He I 10830Å Stokes V and Doppler shifts, coordinated with IRIS Mg II k line profiles and C II Doppler shifts, and Hinode/SP full Stokes fast rasters have the potential to revolutionize our understanding about how these ubiquitous Alfven waves are generated. This can be done by targeting a region toward (but not at) the limb to directly reveal the transverse magnetic field fluctuations associated with Alfven waves, and studying their correlation and phase shifts with photospheric fields (NIRIS, Hinode/SP) and Doppler shifts formed at temperatures in the upper chromosphere (He I 10830Å, Mg II k) and lower transition region (C II 1335Å). Such an analysis has been used successfully (with different spectral lines) to study Alfven waves in the photosphere by (Fujimura and Tsuneta, 2009) but with BBSO's NIRIS we will be able to fully extend this study to the chromosphere where the waves are much stronger and likely more easily generated.

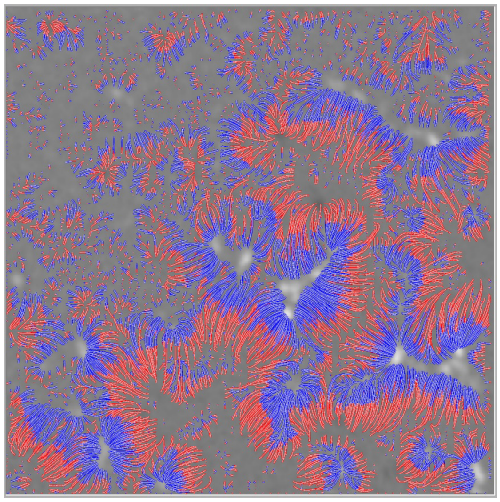

Figure 10: *An example of potential field extrapolation using a quiet Sun HMI data. The open areas are the location of an "open" field lines, i.e., those that left the extrapolation domain. A fraction of a coronal hole is seeing the upper left corner of the FOV, where the loops are shorter and the "open" field areas are larger. The loops change color at the loop apex with the blue half indicating that it originated in positive N polarity fields. Series of field extrapolations using NIRIS magnetograms will allow us to reveal the most dynamic photospheric locations that cause rapid changes in connectivity.*

Photospheric Dynamics and Coronal Heating. The question of coronal heating remains one of the most important and unsolved problems in solar physics. The various models that have been suggested can be divided into two groups: the heating and plasma flows are driven by waves and turbulence propagating along open and large-scale magnetic flux tubes, or alternatively, the source of energy comes from magnetic reconnection between the open/large scale loops and closed loop systems. Cranmer and van Ballegooijen (2010) computed the rate at which closed simulated field lines open up (i.e., recycling times for open flux), and estimated the energy flux released in "reconnection events" involving the opening up of closed flux tubes. They used Monte Carlo simulated "magnetic carpet" and extrapolated the time-varying coronal field. They concluded that in the case of coronal holes the energy flux may be sufficient to power the solar wind, but the field recycling times are far too long to explain the solar wind. Further, quiet Sun regions generate energy fluxes that are too low to be sufficient for solar wind acceleration.

MCAO wide-field corrected, high time cadence NIRIS magnetic field data will allow us to perform a similar study but with a substantial difference: the Monte Carlo simulated "magnetograms" will be replaced with real observed data.

We propose the following: We will use one of the now existing short NIRIS data set to test our numerical tools. We have already developed a numerical tool for that purpose and applied it to and HMI QS and NIRIS pore data sets (Figure 10). We have learned that data/image stability is very important. We will take care of proper alignment, de-stretching, normalization and filtering of the line of sight magnetograms. Then these magnetograms will be used as a boundary condition to calculate potential fields and the field lines. After the MCAO corrected NIRIS data are

collected we will apply the tools to this new data set with a wide FOV and perform potential field extrapolation and analysis. Comparison of extrapolation results based on sequential LOS magnetograms will allow us to detect those locations where field lines changed their connectivity due to new flux emergence, flows, and/or cancellation. We will collect statistics and then use the analysis approach developed by Cranmer and van Ballegooijen (2010) to estimate energy flux and recycling times to test the approach.

Why are *Clear*-NIR data important for this kind of study? The main reason is that MCAO will provide stable seeing over a wide FOV. NIRIS magnetograms, or magnetograms in general, cannot be speckle reconstructed, neither can image selection be performed. The time cadence (40 sec) is two to three times shorter than the lifetime of small-scale magnetic elements that NIRIS resolves and it is sufficient for this kind of study. At this moment GST MCAO is the only tool capable of producing the required data sets. The broader outcome of this work is that such NIRIS datasets, as well as their extrapolation results, will be used for the spicule studies as described below.

Waves in the Chromosphere. The same data set and modeling results will be used to study the origin of various small-scale chromospheric events such as jets and type II spicules. They are short-lived ($<$100 sec), thin ($< 0''.7$) emission structures seen everywhere in Hinode Ca II or Hα images and they show high proper motion velocities, 50-150 km/sec (de Pontieu et al., 2007), twisting motions (De Pontieu et al., 2012) or doubling (Suematsu et al., 2008). Their origin seems to be linked to evolving photospheric magnetic fields (Ji et al., 2012; Yurchyshyn et al., 2013; Martínez-Sykora et al., 2017) and small-scale flux emergence appear to be vital for producing these ubiquitous flows.

Our proposed research is as follows: First, we will use data and results from the previous subsection to address questions of the origin of Type II spicules. For example, the locations where we observe the highest rate of "reconnection" (change of connectivity of the potential field lines) are those where photospheric magnetic fields are the most dynamic. Will these locations also be associated with enhanced production of type II spicules? Another possibility is that the large-scale potential field lines will change not only because of nearby small-scale activity, but also because the underlying cluster of magnetic elements will be deformed by photospheric turbulence. We will be able to pinpoint these locations, as well and compare them to the observed chromospheric activity. We fully realize limitations of the potential field approximation. However, we would like to note that i) we do not intend to reconstruct the realistic magnetic topology, but we are rather using this tool to detect and visualize the most dynamic locations, and ii) the analyzed spatial scales are small and we do not expect to see significant deviation from the potential state, as we typically observe in active regions.

Next, NIRIS chromospheric magnetic field measurements using the10830Å spectral line and refined analysis techniques will be instrumental in studying the role of small-scale magnetic fields in the origin of type II spicules, as well. Even if detailed inversions of the chromospheric fields are difficult and uncertain, the correlation of Stokes parameter fluctuations at the same time and place as a large number of type IIs will tell us if there is a key magnetic factor at work. For example, the cause might be component reconnection of non-parallel, same-polarity fields (Martínez-Sykora et al., 2011), or cancellation of weak transient fields with strong network patches (Moore et al., 2011), or non-linear evolution of propagating waves (Matsumoto and Shibata, 2010) or just appearance of a new flux (Martínez-Sykora et al., 2017). In any case, recent numerical models of type II spicules suggest that chromospheric magnetic field measurements have much more diagnostic power than photospheric fields since the formation mechanism may be intimately tied to the rapid temporal evolution of the field at chromospheric heights (Martínez-Sykora et al., 2011, 2017). MCAO system is vital for this research. Diffraction limited resolution over a wide FOV is essential to detect wave propagation along extended magnetic structures such as large scale, possibly "open" field lines that are thought to originate at small magnetic clusters. (FEEDBACK TO AO???)

C.6 Off-Limb AO and Solar Prominence Study

Introduction. Despite continuing studies of solar prominences, we know little about their physical and magnetic structure on small spatial scales (Labrosse et al., 2010; Mackay et al., 2010; Berger et al., 2017). There are ambiguities related to the broadening of spectral lines of prominences that are attributed to unresolved fine structures (Labrosse et al., 2010). Mackay et al. (2010) outlined several open questions pertaining to prominences among them are the following: 1) Why do different filaments and prominences have very distinct morphologies? and 2) How is prominence plasma/mass supplied and how does it evolve? Moreover, the magnetic structure of prominences and magnetic field-plasma interaction that we observe in these structures are not well understood, as well; and it can only be determined by the inversion of spectro-polarimetric data (Mackay et al., 2010; Mackay and Yeates, 2012).

Berger et al. (2010) identified one specific area that requires further study: quiescent prominences appear to undergo what is known as Rayleigh-Taylor (RT) instability. A loss of equilibrium can lead to plumes of the lighter material pushing up through the denser material and the process is affected by the direction and strength of the mag-

netic field in the prominence. These authors further propose that RT instabilities are one way of replenishing the mass of quiescent prominences, which are constantly draining mass downward. Recent analysis shows that flow shear along the surface of the prominence "bubbles" develops a classic Kelvin-Helmholtz instability that subsequently trigger the RT instability (Berger et al., 2017). Combined, the "bubbles" and drainage flows create a "magneto-thermal convective system" in which hot plasma and presumably magnetic flux are transported into non-potential magnetic field structures with cool plasma draining down to form visible prominence systems. Over time, this convective system may lead to the destabilization of the non-potential magnetic structures to trigger their eruptions as coronal mass ejections (CMEs). The combination of GST, IRIS and Hinode/SOT will be able to probe the prominence bubble phenomenon in much more detail compared to the preliminary studies. The goal is to understand the coronal cavity/quiescent prominence flow system and the evolution into eruptive states; and ultimately, to understand how non-potential magnetic field systems in both quiet-Sun and active regions interact with chromospheric and coronal plasma flows to form filaments, evolve, and eventually erupt as CMEs. More specifically, what causes prominence bubbles? We will measure density and magnetic field gradients along with velocity fields to study the thermodynamics and magnetic structures inherent in these events.

Research. The ability to measure spectra of solar prominences on very fine spatial scales is necessary for understanding solar prominences. There are many ambiguities about prominence behavior with respect to their magnetic fields on small spatial scales because these structures are unresolved (Mackay et al., 2010). Although space-based instruments, such as the SOT on Hinode, can image prominences with high spatial resolution, it is now obvious that the available resolving power is not sufficient to see important details of plasma flows. Moreover, they lack the spectroscopic and polarimetric capabilities necessary to understand prominence dynamics and the nature of the magnetic field which permeates them. Until now, such measurements have been made with ground-based telescopes, but at a resolution limited by the atmosphere.

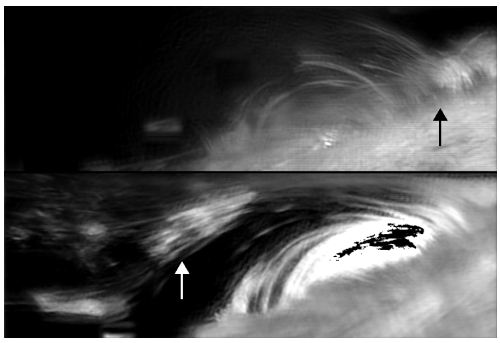

Figure 11: *An active loop prominence as observed in Hα-0.8Å (top) and line center (bottom) spectral lines using GST. The black arrow points toward a dark row of spicules seen against a brighter background of loops. The white arrows indicates fast plasma flows aligned with the coronal magnetic fields.*

We propose to perform the first observations of quiescent solar prominences, active loops, and jets using BBSO's off-limb AO system. We will be using our existing Visible Imaging Spectrometer (VIS) tuned to the H-α spectral line, which is ideal for our purposes. In Figure 11 we show GST Hα-0.8Å and line center (bottom) imges of an active loop prominence that was visible at the edge of the FOV, while a conventional AO system was locked on the granular field in the center of FOV. This prominence displayed fast plasma flows along the field lines creating non-uniform thread like structures (white arrow). The off-band image in the upper panel shows only fractions of that arch but most importantly, one can clearly distinguish dark limb spicules on the brighter background (black arrow). Therefore by locking on a prominence, we will also be able to observe and measure the dynamics of various limb structures such as spicules and jets. Also, Chen (2011) and Joshi et al. (2016) found that certain types of prominence oscillations may be the precursors to CMEs. The solar limb AO system will be able to measure these oscillations with precision, using high resolution, high cadence imaging, coupled with high resolution spectra-polarimetry – a capability which no other system, or spacecraft can match. (Rimmele, Private Communication, 2011) (WHAT ABOUT FISS???)

D. Education, Research Training and Mentoring

Dirk Schmidt, who is an Assistant Scientist at NSO (holds BBSO title of MCAO Project Scientist), is working on the MCAO project and has already worked with Rimmele on prominence AO at the DST, and is a co-PI on this project. In fact he has taken a leadership role as Project Scientist in the AO work at BBSO that is needed in advance of the science proposed here because it builds on his Ph.D. thesis work and his successful work on *Clear*. He is key to enhancing and utilizing the KAOS Evo 2 control software of which he was one of the developers. His work on our utilizing AO in this project will be closely supervised by Goode and Rimmele to ensure he receives needed guidance and support. The mentoring of Schmidt is also discussed in the Supplemental Documents (WHAT TO DO ABOUT THIS SECTION??? DESIGN OF NIR-MCAO CONNECTION TO NIRIS ALSO PLACED THERE) appendage to this proposal.

The data resulting from the proposed experiments with *Clear*-NIR and *Clear*-Prom will be important sources for

Table 1: Tasks and Assignments for the *Clear*-NIR and *Clear*-Prom Projects.

Year	Task	Person(s) In Charge
Year 1	Overall Management and Coordination	Goode and Rimmele
	Project Scientist	Schmidt
	On-sky Experiments in Big Bear	Schmidt, Gorceix and Goode
	Clear-NIR & *Clear*-Prom Control with KAOS Evo 2	Schmidt
	Integration of *Clear*-NIR to NIRIS	Gorceix, Nenow and Cao
	Initial Processing and Checking of Science Data	Yurchyshyn and Ahn
	Data to DKIST SWG & Community	Yurchyshyn
	Interpretation of Scientific Data	Yurchyshyn, Ahn, Rimmele and Goode
Year 2	Overall Management and Coordination	Goode and Rimmele
	Project Scientist	Schmidt
	On-sky *Clear*-NIR & *Clear*-Prom Observations	Schmidt, Gorceix and Goode
	Initial Processing and Checking of Science Data	Yurchyshyn, Ahn and Cao
	System integration of *Clear*-NIR & *Clear*-Prom on GST	Schmidt, Nenow and Gorceix
	Data to DKIST SWG & Community	Yurchyshyn
	Interpretation of Scientific Data	Yurchyshyn, Ahn, Rimmele and Goode
	Regular Observations with *Clear*-NIR & *Clear*-Prom	Team

graduate and undergraduate research. The GST has become a teaching tool for optics, mechanics, computer control and solar physics.

E. GST Data Online and Telescope Time

For this project, we believe that the data should be in the hands of the DKIST SWG, and the community, as soon as possible so as to motivate expanded more detailed DKIST science planning. BBSO has a data pipeline in hand, and will provide prompt announcements of data becoming available to the DKIST team including the SWG, and small, quick look movies will be available to aid the user.

For the observations planned here, both *Clear*-NIR NIRIS and *Clear*-Prom data will be post-processed – dark current and flat field corrections, as well as reconstruction for photometric data and calibration for polarimetric data. To save disk space and download time for "curious users", reduced resolution quick look movies and data sets will be available online (catalog at *http://www.bbso.njit.edu/∼vayur/GST_catalog/* and the automated data request form at *http://www.bbso.njit.edu/∼vayur/nst_requests*). The catalog quick look web page provides detailed information about the data – pointing, observation times, etc. – as well as links to the data request forms allowing one to gain access to FITS files. When one makes an on-line data request, the requested data will appear automatically in an anonymous FTP folder and the requester is emailed the data location. In the special cases in which the data merit keeping the full bursts, the full dataset will also be available without reconstruction. These sets will especially large for MCAO, which generates so much data (e.g., speckle reconstruction reduces the dataset size by about two orders of magnitude). The requested data will appear automatically in an anonymous FTP folder and the requester is emailed the data location. All of these software packages were prepared and written by Vasyl Yurchyshyn.

The observing time of the first, next generation solar telescope in the US, the GST, is already oversubscribed, and will be even more so when it utilizes the various version of *Clear*, and as DKIST comes online because the GST has a unique role of observing in extended campaigns. Further, some DKIST users may well be shunted from DKIST to GST because the smaller aperture may suit the requirements of their observations. We will continue our open data policy, while also making observing time available to the community. The Telescope Allocation Committee ranks the proposals and allocates time. A web page describing all the requests ensures that researchers will not duplicate their data analysis efforts.

E.1 Personnel Management Plan and Timelines - EDIT FROM HERE DOWN???

As of this writing, the preliminary work on the AO for this project has been completed. The GST focal plane instrumentation is mature and for NIR-MCAO the optical setup has been implemented and lab tested with on-sky test to

be done as soon as observing time is available, but well before Summer 2019. The new optical setup looks to the eye indistinguishable from that shown in Fig. 2. Again, the focal plane GST instrumentation to be used here is quite similar to that planned for the DKIST. After all, in the broadest sense the GST is a pathfinder for the DKIST, which accounts for the strong mutual interest in the work proposed here.

The tasks and assignments for the project personnel are listed in Table 1. The project here is relatively straightforward in an organizational sense. The key members of our team are in place. For this project, Goode supervises Kwangsu Ahn, Nicolas Gorceix, Jeff Nenow, and Vasyl Yurchyshyn. Cao is director of BBSO assuring the observing time for the project and was the builder of NIRIS and will be key in integration of MCAO to NIRIS. While, Rimmele supervises the efforts of Dirk Schmidt. In practice, Rimmele and Goode set the overall tasks for the team. Since most of the work is done in Big Bear, when in BBSO Dirk Schmidt supervises the daily experiments in close coordination with Goode and Rimmele. Over the last two decades, Goode and Rimmele have worked on AO-76, AO-308 and MCAO with this broad organizational structure and it works well. **The timelines are crucial here in this two year proposal to provide essential groundwork for DKIST AO/MCAO operations, while motivating early science from DKIST from the outset with the two years planned here ending mid-2021 so there is some overlap with early DKIST observations**.

Dirk Schmidt (co-PI) brings his *Clear* and KAOS system experience and leadership to the project. He already functions well in those roles, while splitting his time between BBSO and NSO/Boulder. Schmidt will spend quartertime on the work proposed here. His presence will make for a seamless technology transfer. Thus, Dirk is the connection between the two essential U.S. solar AO projects − on the GST and DKIST, as Rimmele directs the DKIST project. The close GST-DKIST design similarities ensures that the proposed GST NIR and prominence scientific observations are timely for the implementation of the DKIST science plans.

Nicolas Gorceix, the BBSO optical engineer, has done the double-z MCAO optical design and led its implementation. He already works closely and successfully with Schmidt. As well, Gorceix doubles as an observer during MCAO runs. He will lead the implementation of the optical connection he designed (DESIGN IN SUPPLEMENTAL DOCUMENTS???) to connect *Clear*-NIR to NIRIS. Kwangsu Ahn is expert in obtaining vector polarimetric results from NIRIS data, and as such is essential for bringing the NIRIS data into its full vector richness. He will spend one month a year on this project and will work closely with Vasyl Yurchyshyn. BBSO mechanical engineer, Jeff Nenow will spend one month a year on the fabrication of optical mounts and special setup needs for this project. The *Clear*-Prom setup is already in operation feeding VIS and was used, f.ex., to obtain Fig. 8. Each observing program at BBSO has a Resident Astronomer/Duty Scientist who processes the scientific data to ensure its quality. Vasyl Yurchyshyn has functioned in that role for our project and as a co-PI on this proposal, he will continue to do so. He was the person who setup and implemented the BBSO online data archive (see Sec. **C.5**) and has the broadest experience in examining the quality of BBSO data of anyone at BBSO, and will be essential in making data from this project quickly available to the community. In this effort, he will also organize the NIR MCAO and Prom-AO data for distribution. BBSO (ROLE FOR CAO, IN TABLE???) commits two 10 day observing runs to the *Clear*-NIR and *Clear*-Prom projects during the best parts of the observing season (mid-May to mid-September). Of course, lab experiments can be done anytime during the year, and some on-sky testing can be done any time of year.

E.2 Budget

The requested two year budget for the project is $400 K from the NSF.

The $400 K to BBSO/NJIT will pay one-quarter of Gorceix's salary, one-sixth of the salaries of Yurchyshyn (co-PI) and Goode (PI), and one-twelfth for Kwansu Ahn and Jeff Nenow (mechanical engineer). Vasyl Yurchyshyn is the resident scientist for this project − responsible for initial processing of science data. Rimmele (NSO, co-PI), Cao (BBSO, co-PI) and Berkefeld (Collaborator from KIS, Germany) will be working part-time on this MCAO Project with no charge to the project, as has been done for our earlier AO projects. The budget also includes $4 K per year for travel, which breaks down to $2 K for 2 trips per year from Boulder to Big Bear for Schmidt (co-PI) and $2 K per year for Goode to make two trips per year to Big Bear. All of these trips are for observing runs. BBSO provides free on-site housing for the team during observing runs. Lastly, the budget includes $2 K per year for publication charges. We anticipate 1-2 publications per year.

The sub-award to NSO of $60 K will pay one-quarter of Schmidt's salary (DIRK HOW MUCH TIME WHOULD BE BUDGETED FOR YOU???). Schmidt is the Project Scientist in the work proposed here.

F. References

References

V. Abramenko, V. Yurchyshyn, P. Goode, and A. Kilcik. Statistical distribution of size and lifetime of bright points observed with the new solar telescope. ApJ, 725:L101–L105, December 2010. doi: 10.1088/2041-8205/725/1/L101.

V. I. Abramenko. Dispersion of the solar magnetic flux in the undisturbed photosphere as derived from SDO/HMI data. MNRAS, 471:3871–3877, November 2017. doi: 10.1093/mnras/stx1880.

V. I. Abramenko, V. Carbone, V. Yurchyshyn, P. R. Goode, R. F. Stein, F. Lepreti, V. Capparelli, and A. Vecchio. Turbulent diffusion in the photosphere as derived from photospheric bright point motion. ApJ, 743:133, December 2011. doi: 10.1088/0004-637X/743/2/133.

W. I. Axford, J. F. McKenzie, G. V. Sukhorukova, M. Banaszkiewicz, A. Czechowski, and R. Ratkiewicz. Acceleration of the high speed solar wind in coronal holes. Space Sci. Rev., 87:25–41, January 1999. doi: 10.1023/A:1005197529250.

J. M. Beckers. Increasing the Size of the Isoplanatic Patch with Multiconjugate Adaptive Optics. In *Very Large Telescopes and their Instrumentation*, volume 30 of *European Southern Observatory Conference and Workshop Proceedings*, page 693, 1988.

J. W. Belcher and S. Olbert. Stellar winds driven by alfven waves. ApJ, 200:369–382, September 1975. doi: 10.1086/153798.

T. Berger, A. Hillier, and W. Liu. Quiescent prominence dynamics observed with the hinode solar optical telescope. ii. prominence bubble boundary layer characteristics and the onset of a coupled kelvin-helmholtz rayleigh-taylor instability. ApJ, 850:60, November 2017. doi: 10.3847/1538-4357/aa95b6.

T. E. Berger and A. M. Title. On the relation of g-band bright points to the photospheric magnetic field. ApJ, 553:449–469, may 2001. doi: 10.1086/320663.

T. E. Berger, M. G. Löfdahl, R. A. Shine, and A. M. Title. Measurements of solar magnetic element dispersal. ApJ, 506:439–449, October 1998a. doi: 10.1086/306228.

T. E. Berger, M. G. Löfdahl, R. S. Shine, and A. M. Title. Measurements of solar magnetic element motion from high-resolution filtergrams. ApJ, 495:973–983, March 1998b. doi: 10.1086/305309.

T. E. Berger, G. Slater, N. Hurlburt, R. Shine, T. Tarbell, A. Title, B. W. Lites, T. J. Okamoto, K. Ichimoto, Y. Katsukawa, T. Magara, Y. Suematsu, and T. Shimizu. Quiescent prominence dynamics observed with the hinode solar optical telescope. i. turbulent upflow plumes. ApJ, 716:1288–1307, June 2010. doi: 10.1088/0004-637X/716/2/1288.

T. Berkefeld, D. Soltau, D. Schmidt, and O. von der Lühe. Adaptive optics development at the German solar telescopes. *Applied Optics*, 49:G155, September 2010. doi: 10.1364/AO.49.00G155.

T. Berkefeld, D. Schmidt, D. Soltau, O. von der Lühe, and F. Heidecke. The GREGOR adaptive optics system. *Astronomische Nachrichten*, 333:863, November 2012. doi: 10.1002/asna.201211739.

A. C. Cadavid, J. K. Lawrence, and A. A. Ruzmaikin. Anomalous diffusion of solar magnetic elements. ApJ, 521:844–850, August 1999. doi: 10.1086/307573.

M. P. Cagigal and V. E. Canales. Generalized Fried parameter after adaptive optics partial wave-front compensation. *Journal of the Optical Society of America A*, 17:903–910, May 2000. doi: 10.1364/JOSAA.17.000903.

W. Cao, N. Gorceix, R. Coulter, K. Ahn, T. R. Rimmele, and P. R. Goode. Scientific instrumentation for the 1.6 m new solar telescope in big bear. *Astronomische Nachrichten*, 331:636, June 2010. doi: 10.1002/asna.201011390.

W. Cao, K. Ahn, P. R. Goode, S. Shumko, N. Gorceix, and R. Coulter. The new solar telescope in big bear: Polarimetry ii. In J. R. Kuhn, D. M. Harrington, H. Lin, S. V. Berdyugina, J. Trujillo-Bueno, S. L. Keil, and T. Rimmele, editors, *Solar Polarization 6*, volume 437 of *Astronomical Society of the Pacific Conference Series*, page 345, April 2011.

J. Chae, H.-M. Park, K. Ahn, H. Yang, Y.-D. Park, J. Nah, B. H. Jang, K.-S. Cho, W. Cao, and P. R. Goode. Fast imaging solar spectrograph of the 1.6 meter new solar telescope at big bear solar observatory. Sol. Phys., 288:1–22, November 2013. doi: 10.1007/s11207-012-0147-x.

P. F. Chen. Coronal Mass Ejections: Models and Their Observational Basis. *Living Reviews in Solar Physics*, 8:1, April 2011. doi: 10.12942/lrsp-2011-1.

S. R. Cranmer and A. A. van Ballegooijen. On the generation, propagation, and reflection of alfven waves from the solar photosphere to the distant heliosphere. ApJS, 156:265–293, feb 2005. doi: 10.1086/426507.

S. R. Cranmer and A. A. van Ballegooijen. Can the solar wind be driven by magnetic reconnection in the sun's magnetic carpet? ApJ, 720:824–847, sep 2010. doi: 10.1088/0004-637X/720/1/824.

B. de Pontieu, S. McIntosh, V. H. Hansteen, M. Carlsson, C. J. Schrijver, T. D. Tarbell, A. M. Title, R. A. Shine, Y. Suematsu, S. Tsuneta, Y. Katsukawa, K. Ichimoto, T. Shimizu, and S. Nagata. A tale of two spicules: The impact of spicules on the magnetic chromosphere. PASJ, 59:S655–S662, November 2007. doi: 10.1093/pasj/59.sp3.S655.

B. De Pontieu, S. W. McIntosh, M. Carlsson, V. H. Hansteen, T. D. Tarbell, C. J. Schrijver, A. M. Title, R. A. Shine, S. Tsuneta, Y. Katsukawa, K. Ichimoto, Y. Suematsu, T. Shimizu, and S. Nagata. Chromospheric alfvénic waves strong enough to power the solar wind. *Science*, 318:1574, December 2007. doi: 10.1126/science.1151747.

B. De Pontieu, M. Carlsson, L. H. M. Rouppe van der Voort, R. J. Rutten, V. H. Hansteen, and H. Watanabe. Ubiquitous torsional motions in type ii spicules. ApJ, 752:L12, June 2012. doi: 10.1088/2041-8205/752/1/L12.

A. G. de Wijn, B. W. Lites, T. E. Berger, Z. A. Frank, T. D. Tarbell, and R. Ishikawa. Hinode observations of magnetic elements in internetwork areas. ApJ, 684:1469-1476, September 2008. doi: 10.1086/590237.

R. H. Dicke. Phase-contrast detection of telescope seeing errors and their correction. ApJ, 198:605–615, June 1975. doi: 10.1086/153639.

B. L. Ellerbroek. First-order performance evaluation of adaptive-optics systems for atmospheric-turbulence compensation in extended-field-of-view astronomical telescopes. *Journal of the Optical Society of America A*, 11:783–805, February 1994. doi: 10.1364/JOSAA.11.000783.

R. C. Flicker. Sequence of phase correction in multiconjugate adaptive optics. *Optics Letters*, 26:1743–1745, November 2001. doi: 10.1364/OL.26.001743.

D. Fujimura and S. Tsuneta. Properties of magnetohydrodynamic waves in the solar photosphere obtained with hinode. ApJ, 702:1443–1457, September 2009. doi: 10.1088/0004-637X/702/2/1443.

P. R. Goode, V. Yurchyshyn, W. Cao, V. Abramenko, A. Andic, K. Ahn, and J. Chae. Highest Resolution Observations of the Quietest Sun. ApJ, 714:L31–L35, May 2010. doi: 10.1088/2041-8205/714/1/L31.

P. R. Goode, V. Abramenko, and V. Yurchyshyn. New solar telescope in Big Bear: evidence for super-diffusivity and small-scale solar dynamos? Phys. Scr, 86(1):018402, July 2012. doi: 10.1088/0031-8949/86/01/018402.

R. Ishikawa, S. Tsuneta, Y. Kitakoshi, Y. Katsukawa, J. A. Bonet, S. Vargas Domínguez, L. H. M. Rouppe van der Voort, Y. Sakamoto, and T. Ebisuzaki. Relationships between magnetic foot points and g-band bright structures. *Astron. Astrophys.*, 472:911–918, September 2007. doi: 10.1051/0004-6361:20066942.

H. Ji, W. Cao, and P. R. Goode. Observation of ultrafine channels of solar corona heating. ApJ, 750:L25, May 2012. doi: 10.1088/2041-8205/750/1/L25.

A. D. Joshi, Y. Hanaoka, Y. Suematsu, S. Morita, V. Yurchyshyn, and K.-S. Cho. Pre-eruption Oscillations in Thin and Long Features in a Quiescent Filament. ApJ, 833:243, December 2016. doi: 10.3847/1538-4357/833/2/243.

N. Labrosse, P. Heinzel, J.-C. Vial, T. Kucera, S. Parenti, S. Gunár, B. Schmieder, and G. Kilper. Physics of solar prominences: I - spectral diagnostics and non-lte modelling. Space Sci. Rev., 151:243–332, April 2010. doi: 10.1007/s11214-010-9630-6.

J. K. Lawrence, A. C. Cadavid, and A. Ruzmaikin. Mesogranulation and turbulence in photospheric flows. Sol. Phys., 202:27–39, August 2001. doi: 10.1023/A:1011813925550.

M. Lesieur. Turbulence in fluids: Stochastic and numerical modeling /2nd revised and enlarged edition/. *NASA STI/Recon Technical Report A*, 91, December 1990.

D. H. Mackay and A. R. Yeates. The sun's global photospheric and coronal magnetic fields: Observations and models. *Living Reviews in Solar Physics*, 9:6, November 2012. doi: 10.12942/lrsp-2012-6.

D. H. Mackay, J. T. Karpen, J. L. Ballester, B. Schmieder, and G. Aulanier. Physics of solar prominences: Ii - magnetic structure and dynamics. Space Sci. Rev., 151:333–399, April 2010. doi: 10.1007/s11214-010-9628-0.

Enrico Marchetti, Norbert N. Hubin, Enrico Fedrigo, Joar Brynnel, Bernard Delabre, Robert Donaldson, Francis Franza, Rodolphe Conan, Miska Le Louarn, Cyril Cavadore, Andrea Balestra, Dietrich Baade, Jean-Luis Lizon, Roberto Gilmozzi, Guy J. Monnet, Roberto Ragazzoni, Carmelo Arcidiacono, Andrea Baruffolo, Emiliano Diolaiti, Jacopo Farinato, Elise Vernet-Viard, David J. Butler, Stefan Hippler, and Antonio Amorin. Mad the eso multi-conjugate adaptive optics demonstrator. volume 4839, pages 317–328, 2003. doi: 10.1117/12.458859. URL http://dx.doi.org/10.1117/12.458859.

J. Martínez-Sykora, V. Hansteen, and F. Moreno-Insertis. On the origin of the type ii spicules: Dynamic three-dimensional mhd simulations. ApJ, 736:9, July 2011. doi: 10.1088/0004-637X/736/1/9.

J. Martínez-Sykora, B. De Pontieu, V. H. Hansteen, L. Rouppe van der Voort, M. Carlsson, and T. M. D. Pereira. On the generation of solar spicules and alfvénic waves. *Science*, 356:1269–1272, June 2017. doi: 10.1126/science.aah5412.

T. Matsumoto and K. Shibata. Nonlinear propagation of alfvén waves driven by observed photospheric motions: Application to the coronal heating and spicule formation. ApJ, 710:1857–1867, February 2010. doi: 10.1088/0004-637X/710/2/1857.

S. W. McIntosh, B. de Pontieu, M. Carlsson, V. Hansteen, P. Boerner, and M. Goossens. Alfvénic waves with sufficient energy to power the quiet solar corona and fast solar wind. Nature, 475:477–480, July 2011. doi: 10.1038/nature10235.

A.S. Monin and A.M. Yaglom. *Statistical Fluid Mechanics*, volume 2. MIT Press, Cambridge, MA, 1975.

R. L. Moore, A. C. Sterling, J. W. Cirtain, and D. A. Falconer. Solar x-ray jets, type-ii spicules, granule-size emerging bipoles, and the genesis of the heliosphere. ApJ, 731:L18, April 2011. doi: 10.1088/2041-8205/731/1/L18.

R. Muller, A. Dollfus, M. Montagne, J. Moity, and J. Vigneau. Spatial and temporal relations between magnetic elements and bright points in the photospheric network. *Astron. Astrophys.*, 359:373–380, jul 2000.

B. Neichel, J. R. Lu, F. Rigaut, S. M. Ammons, E. R. Carrasco, and E. Lassalle. Astrometric performance of the Gemini multiconjugate adaptive optics system in crowded fields. MNRAS, 445:500–514, November 2014a. doi: 10.1093/mnras/stu1766.

B. Neichel, F. Rigaut, F. Vidal, M. A. van Dam, V. Garrel, E. R. Carrasco, P. Pessev, C. Winge, M. Boccas, C. d'Orgeville, G. Arriagada, A. Serio, V. Fesquet, W. N. Rambold, J. Lührs, C. Moreno, G. Gausachs, R. L. Galvez, V. Montes, T. B. Vucina, E. Marin, C. Urrutia, A. Lopez, S. J. Diggs, C. Marchant, A. W. Ebbers, C. Trujillo, M. Bec, G. Trancho, P. McGregor, P. J. Young, F. Colazo, and M. L. Edwards. Gemini multiconjugate adaptive optics system review - II. Commissioning, operation and overall performance. MNRAS, 440:1002–1019, May 2014b. doi: 10.1093/mnras/stu403.

M. E. Newington and P. S. Cally. Mode conversion of radiatively damped magnetogravity waves in the solar chromosphere. MNRAS, 417:1162–1169, October 2011. doi: 10.1111/j.1365-2966.2011.19332.x.

Å. Nordlund, R. F. Stein, and M. Asplund. Solar Surface Convection. *Living Reviews in Solar Physics*, 6, December 2009. doi: 10.12942/lrsp-2009-2.

T. J. Okamoto, S. Tsuneta, T. E. Berger, K. Ichimoto, Y. Katsukawa, B. W. Lites, S. Nagata, K. Shibata, T. Shimizu, R. A. Shine, Y. Suematsu, T. D. Tarbell, and A. M. Title. Coronal transverse magnetohydrodynamic waves in a solar prominence. *Science*, 318:1577, December 2007. doi: 10.1126/science.1145447.

R. Ragazzoni, E. Marchetti, and F. Rigaut. Modal tomography for adaptive optics. A&A, 342:L53–L56, February 1999.

F. Rigaut. Ground Conjugate Wide Field Adaptive Optics for the ELTs. In *European Southern Observatory Conference and Workshop Proceedings*, volume 58 of *eso*, page 11, 2002.

F. Rigaut, B. Neichel, M. Boccas, C. d'Orgeville, F. Vidal, M. A. van Dam, G. Arriagada, V. Fesquet, R. L. Galvez, G. Gausachs, C. Cavedoni, A. W. Ebbers, S. Karewicz, E. James, J. Lührs, V. Montes, G. Perez, W. N. Rambold, R. Rojas, S. Walker, M. Bec, G. Trancho, M. Sheehan, B. Irarrazaval, C. Boyer, B. L. Ellerbroek, R. Flicker, D. Gratadour, A. Garcia-Rissmann, and F. Daruich. Gemini multiconjugate adaptive optics system review - I. Design, trade-offs and integration. *Monthly Notices of the Royal Astronomical Society*, 437:2361–2375, January 2014. doi: 10.1093/mnras/stt2054.

F. J. Rigaut, B. L. Ellerbroek, and R. Flicker. Principles, limitations, and performance of multiconjugate adaptive optics. In *Adaptive Optical Systems Technology*, volume 4007 of Proc. SPIE, pages 1022–1031, July 2000.

T. R. Rimmele, F. Woeger, J. Marino, K. Richards, S. Hegwer, T. Berkefeld, D. Soltau, D. Schmidt, and T. Waldmann. Solar multiconjugate adaptive optics at the Dunn Solar Telescope. In *Adaptive Optics Systems II*, volume 7736 of Proc. SPIE, page 773631, July 2010. doi: 10.1117/12.857485.

D. Schmidt, N. Gorceix, P. Goode, J. Marino, T. Rimmele, T. Berkefeld, F. Wöger, and X. Zhang. Multi-conjugate adaptive optics widens the field for observations of the sun. A&A, 597:L8–L11, January 2017. doi: 10.1051/0004-6361/201629970.

D. Schmidt, T.R. Marino, T.R. Rimmele, N. Gorceix, and P.R. Goode. From Clear to DKIST: Advancing solar MCAO from 1.6 meters to 4 meters. In *Adaptive Optics Systems VI*, volume 10703 of Proc. SPIE, 2018a.

D. Schmidt, T.R. Rimmele, N. Gorceix, and J Marino. Wavefront sensing and adaptive optics for solar prominences. In *Adaptive Optics Systems VI*, volume 10703 of Proc. SPIE, 2018b.

Y. Suematsu, K. Ichimoto, Y. Katsukawa, T. Shimizu, T. Okamoto, S. Tsuneta, T. Tarbell, and R. A. Shine. High resolution observations of spicules with hinode/sot. In S. A. Matthews, J. M. Davis, and L. K. Harra, editors, *First Results From Hinode*, volume 397 of *Astronomical Society of the Pacific Conference Series*, page 27, September 2008.

G. E. Taylor, D. Schmidt, J. Marino, T. R. Rimmele, and R. T. J. McAteer. Performance Testing of an Off-Limb Solar Adaptive Optics System. Sol. Phys., 290:1871–1887, June 2015. doi: 10.1007/s11207-015-0697-9.

A. Tokovinin, M. Le Louarn, E. Viard, N. Hubin, and R. Conan. Optimized modal tomography in adaptive optics. A&A, 378:710–721, November 2001. doi: 10.1051/0004-6361:20011213.

S. Tomczyk, S. W. McIntosh, S. L. Keil, P. G. Judge, T. Schad, D. H. Seeley, and J. Edmondson. Alfvén waves in the solar corona. *Science*, 317:1192, August 2007. doi: 10.1126/science.1143304.

D. Utz, A. Hanslmeier, C. Möstl, R. Muller, A. Veronig, and H. Muthsam. The size distribution of magnetic bright points derived from hinode/sot observations. A&A, 498:289–293, April 2009. doi: 10.1051/0004-6361/200810867.

F. Wöger, O. von der Lühe, and K. Reardon. Speckle interferometry with adaptive optics corrected solar data. A&A, 488:375–381, September 2008. doi: 10.1051/0004-6361:200809894.

V. Yurchyshyn, V. Abramenko, and P. Goode. Dynamics of Chromospheric Upflows and Underlying Magnetic Fields. ApJ, 767:17, April 2013. doi: 10.1088/0004-637X/767/1/17.